Am J Physiol Gastrointest Liver Physiol 306: G1–G12, 2014.
First published October 31, 2013; doi:10.1152/ajpgi.00263.2013.

Acute interactions between intestinal sugar and calcium transport in vitro

Phuntila Tharabenjasin,[1,2,3] Veronique Douard,[1] Chirag Patel,[1] Nateetip Krishnamra,[2,3] Richard J. Johnson,[4] Jian Zuo,[5] and Ronaldo P. Ferraris[1]

[1]*Department of Pharmacology and Physiology, Rutgers Biomedical and Health Sciences, New Jersey Medical School (NJMS), Newark, New Jersey;* [2]*Exercise Science Graduate Program, Department of Physiology, and* [3]*Center of Calcium and Bone Research (COCAB), Faculty of Science, Mahidol University, Bangkok, Thailand;* [4]*The Division of Renal Diseases and Hypertension, Department of Medicine, University of Colorado, Aurora, Colorado;* [5]*Department of Developmental Neurobiology, St. Jude Children's Research Hospital, Memphis, Tennessee*

Submitted 12 August 2013; accepted in final form 24 October 2013

Tharabenjasin P, Douard V, Patel C, Krishnamra N, Johnson RJ, Zuo J, Ferraris RP. Acute interactions between intestinal sugar and calcium transport in vitro. *Am J Physiol Gastrointest Liver Physiol* 306: G1–G12, 2014. First published October 31, 2013; doi:10.1152/ajpgi.00263.2013.—Fructose consumption by Americans has increased markedly, whereas Ca^{2+} intake has decreased below recommended levels. Because fructose metabolism decreases enterocyte ATP concentrations, we tested the hypothesis that luminal fructose acutely reduces active, diet-inducible Ca^{2+} transport in the small intestine. We confirmed that the decrease in ATP concentrations was indeed greater in fructose- compared with glucose-incubated mucosal homogenates from wild-type and was prevented in fructose-incubated homogenates from ketohexokinase $(KHK)^{-/-}$ mice. We then induced active Ca^{2+} transport by chronically feeding wild-type, fructose transporter glucose transporter 5 $(GLUT5)^{-/-}$, as well as $KHK^{-/-}$ mice a low Ca^{2+} diet and measured transepithelial Ca^{2+} transport in everted duodenal sacs incubated in solutions containing glucose, fructose, or their nonmetabolizable analogs. The diet-induced increase in active Ca^{2+} transport was proportional to dramatic increases in expression of the Ca^{2+}-selective channel transient receptor potential vanilloid family calcium channel 6 as well as of the Ca^{2+}-binding protein 9k (CaBP9k) but not that of the voltage-dependent L-type channel Ca(v)1.3. Crypt-villus distribution of CaBP9k seems heterogeneous, but low Ca^{2+} diets induce expression in more cells. In contrast, KHK distribution is homogeneous, suggesting that fructose metabolism can occur in all enterocytes. Diet-induced Ca^{2+} transport was not enhanced by addition of the enterocyte fuel glutamine and was always greater in sacs of wild-type, $GLUT5^{-/-}$, and $KHK^{-/-}$ mice incubated with fructose or nonmetabolizable sugars than those incubated with glucose. Thus duodenal Ca^{2+} transport is not affected by fructose and enterocyte ATP concentrations but instead may decrease with glucose metabolism, as Ca^{2+} transport remains high with 3-*O*-methylglucose that is also transported by sodium-glucose cotransporter 1 but cannot be metabolized.

calbindin; fructose; glucose; glucose transporter 5; metabolism; nutrition

INTESTINAL CALCIUM TRANSPORT has saturable and nonsaturable components and may be passive and paracellular or active and transcellular (6, 8, 16, 32, 40). Transepithelial active Ca^{2+} transport across the enterocyte occurs mainly in the proximal intestine and is thought to consist of three major steps, which are *1*) passive Ca^{2+} entry mainly via the Ca^{2+}-selective channel, transient receptor potential vanilloid family calcium channel 6 (TRPV6), on the apical membrane, *2*) Ca^{2+} translocation across the cytoplasm with Ca^{2+}-binding protein D_9K (CaBP9k, calbindin), and *3*) active Ca^{2+} extrusion from the enterocyte to the blood by the plasma membrane Ca^{2+}-ATPase isoform 1b (PMCA1b) and the Na^+/Ca^{2+} exchanger isoform 1 (NCX1) (40). Thus the basolateral exit step requires energy either directly via ATP hydrolysis or indirectly via the Na^+ gradient. Active transepithelial Ca^{2+} transport mediated primarily by these transporters is typically very low in adult mammals consuming diets containing normal Ca^{2+} levels but can be induced mainly in the duodenum by $1,25(OH)_2D_3$ during chronic physiological (e.g., growth, pregnancy, and lactation) and nutritional (e.g., dietary Ca^{2+} deficiency) Ca^{2+} stress (6, 8, 16, 32, 40). This study used low-Ca^{2+}, vitamin D-sufficient diets to upregulate Ca^{2+} transporter activity in the duodenum and is thus concerned primarily with acute effects of sugars on diet-inducible, $1,25(OH)_2D_3$-regulated, active Ca^{2+} transport.

Because it is important for intracellular signaling and for the regulation of cardiac and muscle activity, Ca^{2+} concentrations in the blood are tightly regulated within a very narrow range, so acute deficiencies are quickly addressed at the expense of Ca^{2+} stores in the skeleton, whereas chronic deficiencies are typically resolved by adaptive increases in active Ca^{2+} transport in the small intestine and kidney. Intestinal Ca^{2+} absorption may depend, not only on dietary Ca^{2+} and serum vitamin D concentrations, but also on dietary factors that may alter luminal Ca^{2+} concentrations or interfere with Ca^{2+} transporters. Dietary factors that have been shown to affect Ca^{2+} bioavailability include plant fiber, fat, phosphorus, protein, and carbohydrate (1, 2, 9, 35). Concerning potential interactions between intestinal carbohydrate and Ca^{2+} absorption, most investigations have focused on the stimulating effect of the milk sugar lactose on the absorption of Ca^{2+} (3, 14, 27, 51, 52), as these two nutrients are typically in the intestinal lumen at the same time. Moreover, monosaccharides such as glucose and/or galactose have also been reported to acutely affect intestinal Ca^{2+} transport (11, 60, 69, 75). There have only been a few studies that evaluated the direct effect of fructose on Ca^{2+} absorption (3, 69), but these early pioneering studies used high luminal fructose concentrations (550 and 160 mM) and were conducted using sacs of the rat ileum, which expresses few transporters and thus exhibits little active Ca^{2+} transport (8). More importantly, none of these studies studied the acute effects of sugars on that component of Ca^{2+} transport that is diet-inducible and thus important during periods of physiological and nutritional Ca^{2+} stress.

Like diet-inducible active Ca^{2+} transport, sugar transport also occurs mainly in the proximal intestine (29). Apical glu-

Address for reprint requests and other correspondence: R. Ferraris, Dept. of Pharmacology & Physiology, Rutgers Biomedical and Health Sciences, New Jersey Medical School (NJMS), 185 South Orange Ave., Newark, NJ 07103 (e-mail: ferraris@njms.rutgers.edu).

cose and galactose sodium-glucose cotransporter 1 (SGLT1)-mediated transport into the cell is active and electrogenic (72). Depending primarily on the nutritive status of the body, glucose can be metabolized but is generally accumulated to a high concentration in the cytosol for the facilitative glucose transporter 2 (GLUT2)-mediated downhill transport into the blood containing ~5 mM glucose (15, 44). In contrast, transepithelial fructose absorption is entirely passive. Uptake across the apical membrane is mediated by GLUT5, whereas basolateral exit is mediated by GLUT2 (53, 65). Fructose is not bound to any protein during transit across the cytosol but can be metabolized in the enterocytes (33, 54). Compared with glucose metabolism, which is highly regulated, fructose catabolism is irreversibly initiated by the ketohexokinase (KHK, also known as fructokinase) enzyme, which produces fructose-1-phosphate (19, 38). After fructose uptake, fructose-1-phosphate is rapidly accumulated, whereas creatine phosphate, ATP, or intracellular Pi concentrations are reduced in the enterocyte (33, 38, 45, 49, 54). The mechanism underlying the depletion of energy-rich intermediates and accumulation of fructose-1-phosphate is thought to be the relatively slow activity of downstream enzymes that further catabolize fructose-1-phosphate, compared with that of KHK (68, 71).

How can transport between Ca^{2+} and fructose, or between Ca^{2+} and glucose, possibly interact, as their intestinal absorption involves completely different apical, intracellular, and basolateral proteins? This question is timely because a growing number of modern dairy products that are used as primary nutritive Ca^{2+} sources (55) is now sweetened with high-fructose corn syrups (HFCS), which usually contain 55% fructose and 45% glucose (36). Moreover, fructose consumption rates have increased dramatically such that fructose now constitutes ~10% of daily energy intake (23), whereas Ca^{2+} intake by Americans has decreased markedly to levels below recommended (7, 55). Likewise, glucose constitutes about half of HFCS and, the table sugar sucrose is the end product of luminal starch digestion and can reach average luminal concentrations of ~48 mM that may be high enough as to affect Ca^{2+} transport (31). We have previously shown fructose concentrations from luminal fluids to average ~25 mM (43). These substantial sugar concentrations increase the importance of identifying mechanisms by which luminal sugars can acutely compromise Ca^{2+} transport.

Because intestinal fructose metabolism can markedly reduce intracellular ATP concentrations, we tested the hypothesis that fructose acutely reduces transcellular active Ca^{2+} transport in the small intestine and predicted that Ca^{2+} transport should be normal in GLUT5$^{-/-}$ and KHK$^{-/-}$ mice that cannot absorb and metabolize, respectively, dietary fructose.

MATERIALS AND METHODS

Animal and experimental design. Male C57BL/6 wild-type mice weighing 13–15 g (4 wk old) were obtained from Taconic (Germantown, NY) and housed in the Research Animal Facility of the NJMS in a temperature-controlled room of 22–24°C with a 12-h:12-h light/dark cycle. Mice were fed on a regular laboratory nonpurified diet (Purina Mills, Richmond, IN) and had access to water ad libitum before the beginning of the experiment. Both KHK$^{-/-}$ (lacking both ketohexokinase isoforms A and C) and GLUT5$^{-/-}$ mice have the same background strain as wild-type. Generation of KHK$^{-/-}$ (19) and GLUT5$^{-/-}$ (73) are as described in detail previously. Intestines from CaBP9k$^{-/-}$ mice were a generous gift from Prof. Sylvia Christakos of the New Jersey Medical School. All of the procedures conducted in this study were approved by the Institutional Animal Care and Use Committee of NJMS.

In this study, all mice used for transport studies were chronically fed either a low- or normal-Ca^{2+} diet, and dietary carbohydrate content was similar in both diets. Thus 4-wk-old wild-type, KHK$^{-/-}$, and GLUT5$^{-/-}$ mice were each divided into two groups and fed either with normal-Ca^{2+} (0.5% Ca^{2+} diet; D10122104 based on AIN-93M; Research Diets, New Brunswick, NJ) or low-Ca^{2+} diet (0.02% Ca^{2+}; D11040807) for 4 wk. Our proximate analysis confirmed these Ca^{2+} levels and also indicated that concentrations of phosphate and other electrolytes were the same in both diets. Active intestinal Ca^{2+} transport was determined using the everted gut sac assay described below, in the presence of various sugars added in the incubation medium. Tissue was also harvested, and RNA was isolated for quantification of gene expression by real-time PCR.

As we were comparing in some experiments the acute effects of different sugars on diet-inducible Ca^{2+} transport, these experiments only utilized mice fed a low-Ca^{2+} diet and thus exhibited high rates of Ca^{2+} transport. We first had to demonstrate that wild-type, GLUT5$^{-/-}$, and KHK$^{-/-}$ mice were equally capable of upregulating Ca^{2+} transport when fed a low-Ca^{2+} diet. Breeding of KHK$^{-/-}$ and of GLUT5$^{-/-}$ mice was completely unpredictable, and the sex ratio varied markedly between litters; thus whenever we were able to wean two same-age KHK$^{-/-}$ or GLUT5$^{-/-}$ males, one would be fed a normal-Ca^{2+} and the other a low-Ca^{2+} diet for 4 wk, and then Ca^{2+} transport would be determined as described below. Because diet-inducible, active Ca^{2+} transport is age dependent, we used age-matched mice in all experiments.

When it was shown that upregulation by low-Ca^{2+} diet was the same in all three genotypes, we studied the acute effects of glucose and fructose on this inducible component of Ca^{2+} transport. Whenever we were able to wean two same-age KHK$^{-/-}$ or GLUT5$^{-/-}$ males, both were fed low-Ca^{2+} diets, and, after 4 wk, Ca^{2+} transport was determined in the presence of glucose in one duodenal sac from one mouse and in the presence of fructose in another sac from another mouse.

In vitro intestinal Ca^{2+} transport. Mice were weighed and anesthetized by an i.p. injection of 2–4 ml/kg body wt of a mixture of ketamine (20 mg/ml) and xylazine (2.5 mg/ml). Intestinal Ca^{2+} transport was determined using the classical everted gut sac method, following protocols validated using TRPV6/CaBP-null (double deletion) mice by Benn et al. (5) and described in detail by others (6, 8), who showed that the everted gut sac assay selectively measures active intestinal Ca^{2+} transport because the Ca^{2+} transport is against a concentration gradient, occurs at low concentrations of Ca^{2+}, and is saturable. In fact, many kinetic characteristics of Ca^{2+} transport determined by the everted sac method are in many respects similar to those of observed in vivo (26, 59). We also showed that Ca^{2+} transport in uneverted compared with everted sacs is low and likely paracellular (25). We used the everted sac as many studies on Ca^{2+} transport have used this method. Only one everted sac from the duodenum could be taken per animal. We used the duodenum because *1*) active, diet-inducible Ca^{2+} transport decreases markedly in more distal intestinal regions and *2*) fructose and glucose absorption are greater in the duodenum and proximal jejunum than in more distal regions (6, 12, 25, 28).

The first 7 cm of the proximal duodenum was removed, rinsed with ice-cold Ca^{2+} transport buffer [(in mM) 125 NaCl, 11.3 HEPES, and 0.25 $CaCl_2$, pH = 7.4, osmolality = 280 mOsm/kg], and then slowly everted by rolling the segment along the stainless steel rod. The everted intestinal segment was filled with 500 μl of Ca^{2+} transport buffer with 10 mM glucose, fructose, or sugar analogs that was trapped inside by tying threads on both ends. The sugar concentration of 10 mM was based on our previous findings on average total intestinal luminal glucose and fructose (0.4–26 mM) concentrations

that can reach up to 48 mM in the duodenum during peak feeding times (31, 43). The sacs were incubated in test tubes with exactly the same incubation buffer as that inside the sac, plus $^{45}CaCl_2$ (40,000 cpm/ml). After 1 h, the intact sacs were removed, and 50 μl of serosal fluid were collected and then analyzed for $^{45}Ca^{2+}$ in Ecolume (a premixed liquid scintillation cocktail, MP Biomedical, Solon, OH), using a liquid scintillation counter (Beckman LS6500; Beckman, Fullerton, CA). The active accumulation of $^{45}Ca^{2+}$ inside the sac was expressed as a ratio of the final concentration of $^{45}Ca^{2+}$ inside (serosal compartment) and $^{45}Ca^{2+}$ outside (mucosal compartment). After the removal 50 μl from the serosal compartment for counting, excess fluid was drained from the sac, and the tissue was blotted dry, weighed, and digested using Solvable (PerkinElmer, Waltham, MA) at 37°C for 24 h before $^{45}Ca^{2+}$ determination. $^{45}Ca^{2+}$ accumulated in the tissue was divided by the weight of the empty sac.

In some studies, the ratio of $^{45}Ca_{in}/^{45}Ca_{out}$ in mice fed a low-Ca^{2+} diet was expressed relative to those fed normal Ca^{2+} for experiments done the same day. This was necessary because breeding of $KHK^{-/-}$ and $GLUT5^{-/-}$ mice was not predictable, and thus experiments could not be done with wild-type mice. In turn, Ca^{2+} transport in sacs from mice fed the normal-Ca^{2+} diet was normalized to average values from multiple experiments (see Fig. 3). Once we demonstrated that a low-Ca^{2+} diet induced Ca^{2+} transport in intestines from wild-type, $CaBP9k^{-/-}$, and $GLUT5^{-/-}$ mice, we then used mice fed only low Ca^{2+} to determine the effect of acute glucose or fructose incubation on the diet-inducible component of Ca^{2+} transport (see Fig. 6). Here, the ratio of $^{45}Ca_{in}/^{45}Ca_{out}$ in intestines incubated with fructose was expressed relative to those incubated with glucose for experiments done the same day. Ca^{2+} transport in sacs incubated with glucose was normalized to average values from multiple experiments (see Fig. 6). Regarding experiments that used only wild-type mice, no normalization was made, and absolute values are presented, as Ca^{2+} transport was determined in all treatments simultaneously.

ATP measurement in the intestinal mucosa. Intracellular ATP concentration was determined using a rapid bioluminescence ATP assay kit according to the manufacturer's instructions (EnzyLight ATP assay kit; BioAssay Systems, Hayward, CA). With the use of instruments kept ice-cold in the freezer and ice-cold solutions, ~20 cm of the proximal small intestine was flushed with ice-cold PBS (pH 7.4). The mucosa was quickly scraped on a glass slide on ice, suspended in ice-cold HEPES-buffered balanced salt solution (in mM, 25 HEPES, 121 NaCl, 5 $NaHCO_3$, 4.7 KCl, 1.2 $MgSO_4 \cdot 7H_2O$, 1.1 phosphate, and 2 $CaCl_2$, pH 7.4), and mixed by gentle inversions of test tubes encased in ice. A 125-μl aliquot was then pipetted and incubated in 125 μl of sugar solution (also dissolved in ice-cold HEPES-buffered balanced salt solution) as instructed (final concentration = 5.5 mM) for 5 min at 37°C. Thus the concentrations of the other components were not changed after 1:1 dilution.

After incubation, the entire sample was immediately transferred into 250 μl of 0.2 M trichloroacetic acid solution and homogenized by a tissue grinder (IKA Ultra-Turrax T25 Basic Homogenizer; IKA Works, Wilmington, NC) on ice. The supernatant was separated by centrifugation at 12,000 *g* for 5 min at 4°C. Two 50-μl aliquots of samples were kept in −80°C until further analyses for protein levels. To measure the ATP level, the supernatant was first buffered with 25 μl of 0.2 M NaOH solution, and then 10 μl of sample was transferred in duplicate into 96-well white opaque plates (PerkinElmer Life Sciences). Each well contained 90 μl of a reconstituting reagent containing a mixture of assay buffer, *D*-luciferin, and luciferase enzyme at a ratio of 95:1:1 (vol/vol/vol). Luminescence was read against blanks (buffer without sample) using an automated microplate reader (Multilabel HTS Counter; VICTOR, Wallac, Finland) (67). Protein levels were quantified by BCA protein assay kit (Pierce ThermoFisher Scientific, Rockford, IL), using bovine serum albumin as a protein standard. ATP concentration was normalized to per milligram of protein.

Total mRNA extraction, DNase treatment, and RT reaction. Total RNA was extracted using a commercially available TRIZOL reagent (Invitrogen, Carlsbad, CA). To hydrolyze contaminating DNA in RNA preparation, 100 μg RNA was combined with 10 μl DNase I and 70 μl RDD buffer (RNeasy Mini Kit; Qiagen, Valencia, CA) in a final volume of 100 μl. The cDNA was generated from 5 μg DNase-treated RNA using 200 U of SuperScript III RNase H Reverse Transcriptase and oligo (dT) 20 (Invitrogen) in a total volume of 20 μl.

Gene expression by real-time PCR. Real-time PCR was performed using Mx3000P (Stratagene Real-Time PCR System, La Jolla, CA), as described previously (21). Primers were designed using Roche primer design software (http://www.roche-applied-science.com) and were purchased from Integrated DNA Technologies (IDT, Coralville, IA) (Table 1). The relative ratio of expression levels of target genes was calculated as described previously (63). Gene expression was relative to elongation factor-1α gene, whose expression was previously found to be independent of Ca^{2+} level in the diet and of age of the mice.

Immunohistochemistry. Two centimeters of mouse duodenum were excised and immediately fixed in fresh 10% paraformaldehyde in PBS (pH = 7.35) overnight at room temperature (25°C). After fixation,

Table 1. *Primer sequences of genes whose expression level had been measured by real-time PCR*

Gene Name (symbol)	Accession No.	Direction	Primer Sequences (5′→3′)
Transient receptor potential cation channel, subfamily V, member 6 (TRPV6)	NM_022413.3	Forward	5′-GCTGATGGCTGTGGTAATTCT-3′
		Reverse	5′-GGGATCCTCTGTCTGGAAAA-3′
Calcium-binding protein D9k (CaBP9k)	NM_009789.2	Forward	5′-AAATATGCAGCCAAGGAAGG-3′
		Reverse	5′-CAGCTCCTTAAAGAGATTGTCCA-3′
Plasma calcium transporting membrane ATPase 1 (PMCA1)	NM_026482.2	Forward	5′-TGACGATGAACAGGATGACG-3′
		Reverse	5′-CCAAGAGAAACCCCAACAAG-3′
Solute carrier family 8 (sodium/calcium exchanger) member 1 (NCX1)	NM_001112798.1	Forward	5′-TGTGTGCTTCTGTTGGTGGT-3′
		Reverse	5′-GATAAATGGGCTGTGCTTGG-3′
Glucose transporter 5 (GLUT5)	AF233337.1	Forward	5′-TGCAGAGCAACGATGGAGAAA-3′
		Reverse	5′-ACAGCAGCGTCAGGGTGAAG-3′
Glucose transporter 2 (GLUT2)	X78722.1	Forward	5′-ATCGCTCCAACCACACTC-3′
		Reverse	5′-CCTGACTTCCTCTTCCAACT-3′
Ketohexokinase (KHK)	NM_008439.3	Forward	5′-AACTCCTGCACTGTCCTTTCCTT-3′
		Reverse	5′-CCACCAGGAAGTCGGCAA-3′
Sodium/glucose cotransporter member 1 (SGLT1)	NM_019810.4	Forward	5′-GCCGAAGTATGGTGTGGT-3′
		Reverse	5′-TTGTGAAGATGTAGAGGAGCAG -3′
Voltage-gated dependent calcium channel pore forming α1 subunit (Ca(v)1.3)	AF370010	Forward	5′-GCAGAGTTGTAAGTGCGGTAGA-3′
		Reverse	5′-TCTTGCATAGTTTGCCTCTGC -3′
Eukaryotic translation elongation factor 1 α1 (Ef1α1)	NM_010106.2	Forward	5′-ACACGTAGATTCCGGCAAGT-3′
		Reverse	5′-AGGAGCCCTTTCCCATCTC-3′

tissue samples were embedded in paraffin, then sectioned (~5 μm), deparaffinized, and rehydrated as previously described (22). Antigen unmasking was processed in 10 mM sodium citrate buffer (pH 6.0) solution in heat-induced antigen retrieval programmed pressure cooker (2100-Retriever; ProteoGenix, Schiltigheim, France). Slices were washed in sterile water and then blocked with 1% normal goat serum for 1 h at room temperature. Tissue sections were incubated in primary antibody in dark humidified chamber; chicken anti-KHK (1:200; Sigma-Aldrich, St. Louis, MO), and rabbit anti-Calbindin D-9k (1:1,000; Swant Swiss Antibodies, Bellinzona, Switzerland) in diluted in 1% normal goat serum overnight at 4°C. The section was then washed in PBS three times at 10 min each. Fluorochrome-labeled secondary antibodies [DyLight 488-conjugated AffiniPure donkey anti-chicken IgG (1:400; Jackson ImmunoResearch, West Grove, PA) for KHK and Cy™3 goat anti-rabbit IgG (Chemicon International, Temecula, CA) for CaBP9k (1:200)] were applied for 1 h at room temperature. After incubation, tissues were washed again in PBS and mounted with fluorescent mounting medium (Dako North America, Carpenteria, CA). The stained sections were examined at ×20 with a laser scanning confocal microscope (Nikon Eclipse Ti; NIS-Elements AR 4.11.00 program). All images of sections being compared were obtained with the same settings of the microscope. Nonspecific staining with secondary antibodies alone was consistently negligible. The KHK and CaBP9k antibodies did not stain sections from $KHK^{-/-}$ and $CaBP9k^{-/-}$ mice, respectively.

Statistical analyses. Data are presented as means ± SE. A two-way ANOVA analyzed the effects of genotype and diet or of genotype and incubation solution. When a two-way ANOVA could not be used, a one-way ANOVA was utilized to determine the difference among groups with different treatments. If there was a significant difference, Fisher's paired least significant difference test was used (STATVIEW; Abacus Concepts, Piscataway, NJ) to determine differences among means. Differences were considered significant at $P < 0.05$. Graphs were plotted by GraphPad Prism 5.0 (GraphPad Software, San Diego, CA).

RESULTS

Fructose decreases intracellular ATP concentration in wild-type but not in $KHK^{-/-}$ mice. In preliminary work, we determined ATP concentrations in mucosal homogenates incubated in fructose and glucose for up to 20 min (not shown) and found that the rate of ATP reduction was linear for ≤5 min, a time course used in the next series of experiments. Initial ATP concentrations were 47.1 ± 1.4 nmol/mg of protein and did not differ significantly among glucose- and fructose-incubated mucosal homogenates from wild-type and $KHK^{-/-}$ mice. After incubation of mucosal homogenates with glucose or fructose solutions, ATP concentrations decreased from initial at a rate of ~14%/min in glucose-incubated mucosal homogenates of wild-type mice (Fig. 1*A*). Fructose incubation further reduced ATP levels, so the concentration remaining was only 7.9 ± 0.32% of initial or about half of that remaining in glucose-incubated mucosa. By two-way ANOVA, the effects of KHK deletion and of sugar incubation on ATP levels were highly significant ($P = 0.005$ and 0.02, respectively). The interaction between genotype and sugar treatments was also significant ($P = 0.0316$), suggesting that fructose-induced ATP reduction depended on genotype. The difference between glucose and fructose effects on ATP concentrations in wild-type mice was highly significant ($P < 0.001$). In contrast, in $KHK^{-/-}$ mice, the amount of ATP left was similar between fructose- and glucose-incubated mucosa. Increasing the incubation time further reduced ATP levels, but the fructose-incubated mucosa from wild-type mice still had the greatest decrease (Fig. 1*B*). By two-way ANOVA, the effects of KHK deletion and of fructose incubation on ATP levels were still significant at 9 min ($P = 0.003$ and 0.05, respectively). The interaction between genotype and sugar solution was not significant ($P = 0.10$) although a post hoc *t*-test between glucose and fructose effects in wild-type mice was highly significant ($P < 0.01$). Although this finding merely confirms earlier work indicating marked reductions in enterocyte ATP levels with fructose (33, 38, 48, 54), it does show for the first time that KHK may be the major reason for this marked decrease in ATP levels in intestinal mucosa exposed to fructose.

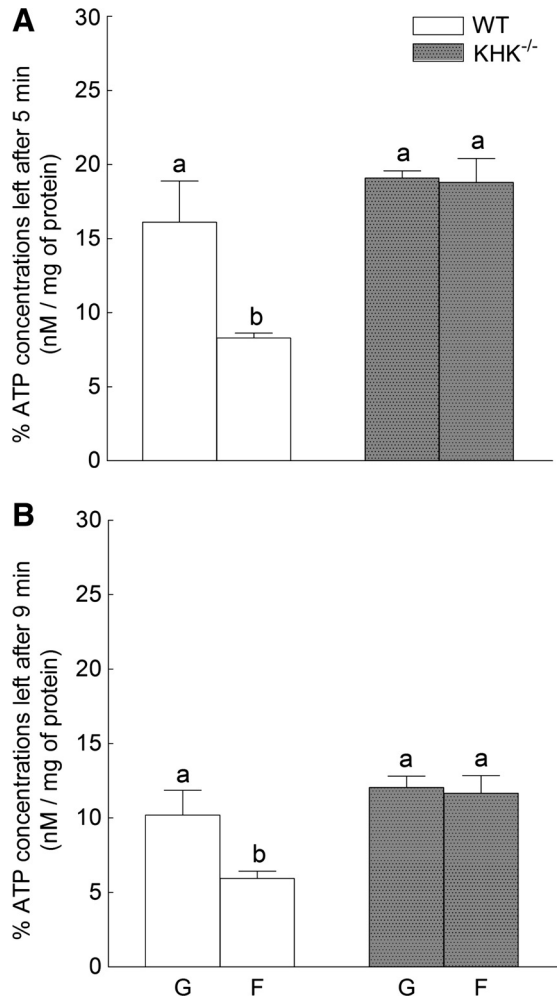

Fig. 1. Changes in intracellular ATP levels after incubation with 5.5 mM glucose (G) or fructose (F). Intestinal mucosa from wild-type (WT) and ketohexokinase (KHK)$^{-/-}$ mice fed commercial chow were scraped then placed on glass slides on ice, homogenized in ice, and then incubated in glucose or fructose solutions for 5 and 9 min at 37°C following kit manufacturer instructions. Intracellular ATP concentrations were determined by a rapid bioluminescent method. Values are means ± SE ($n = 3$–4). Different letters denote significant ($P < 0.05$) differences. KHK-mediated fructose metabolism reduces ATP concentrations in intestinal mucosal homogenates.

CaBP9k and KHK are expressed in the small intestine. We have previously shown GLUT5 protein (25) and mRNA (42) to be expressed in enterocytes lining the villi, especially near the tip. Before testing our hypothesis, we wanted to demonstrate that CaBP9k is found in cells where KHK-mediated fructose metabolism occurs. KHK is clearly found in enterocytes along

the villus axis of the duodenum (Fig. 2*A*) as well as that of the ileum (Fig. 2*B*). The KHK antibody is specific, as indicated by the absence of immunofluorescence in wild-type mice probed with secondary antibody alone, and in KHK$^{-/-}$ mice probed with both primary and secondary antibodies (Fig. 2*E*). CaBP9k distribution is similar to that of KHK in wild-type mice fed low-Ca^{2+} diets (Fig. 2*A*). However, in wild-type mice fed a normal-Ca^{2+} diet (Fig. 2*C*), there was a marked reduction in CaBP9k immunofluorescence, and CaBP9k was expressed in only a few cells (see merged panel). In mice fed low Ca^{2+}, there seems to be a regional gradient of CaBP9k expression as levels decrease in the ileum (compare Fig. 2*A*, *left* with Fig. 2*B*, *left*).

CaBP9k distribution was also heterogeneous and seemingly punctuate, with some cells expressing more immunoreactive protein than others, along the intestinal villus axis of GLUT5$^{-/-}$ (not shown) and KHK$^{-/-}$ mice (Fig. 2*F*, *left*) as well as of rats (Fig. 2*F*, *right*) fed normal-Ca^{2+} diets. The CaBP9k antibody has also been shown to be highly specific as indicated by negative controls of intestinal sections from wild-type (probed with secondary antibody only) and CaBP9$^{-/-}$ (probed with both primary and secondary antibodies) mice (Fig. 2*D*).

Low-Ca^{2+} diets increased Ca^{2+} transport as well as TRPV6 and CaBP9k expression. When fed a low-Ca^{2+} diet, mice of all three genotypes clearly exhibited large adaptive increases of 60–100% in transepithelial (ratios of $^{45}Ca_{in}/^{45}Ca_{out}$; Fig. 3*A*) and in transmembrane (amounts of $^{45}Ca^{2+}$ accumulated in tissues; Fig. 3*B*) transport of 0.25 mM Ca^{2+}. This adaptive increase in transepithelial and transmembrane Ca^{2+} transport induced by Ca^{2+}-deficient diets has been shown to be active, $1,25(OH)_2D_3$ dependent, and mediated mostly by TRPV6 and CaBP9k (5, 6, 8, 24, 25).

The absolute ratios of $^{45}Ca_{in}/^{45}Ca_{out}$ in mice fed normal Ca^{2+} were 0.46 ± 0.04 for wild-type, 0.51 ± 0.05 for GLUT5$^{-/-}$, and 0.47 ± 0.03 for KHK$^{-/-}$ (Fig. 3*A*). The amounts of $^{45}Ca^{2+}$ accumulated in tissues were 39.9 ± 3.2 for wild-type, 38.0 ± 2.8 for GLUT5$^{-/-}$, and 43.8 ± 2.4 × 10^3 cpm/g tissue for KHK$^{-/-}$ mice (Fig. 3*B*). Because experiments could not be conducted at the same time across genotype, Ca^{2+} transport in sacs from mice fed low Ca^{2+} were subsequently normalized to those in sacs from mice fed normal Ca^{2+} levels for each genotype. When analyzed by two-way ANOVA, genotype had no effect on normalized transepithelial (P = 0.17) and transmembrane (P = 0.62) Ca^{2+} transport. In contrast, diet had a dramatic effect ($P < 0.0001$ for Fig. 3, *A* and *B*), but there was no interaction between genotype and diet ($P \geq 0.28$).

The increases in Ca^{2+} transport were paralleled by dramatic 30- to 40-fold increases in mRNA expression of known major players of Ca^{2+} transport (40). Relative TRPV6 and CaBP9k mRNA expression were significantly upregulated by diet ($P <$ 0.0001 by two-way ANOVA) in intestines of wild-type,

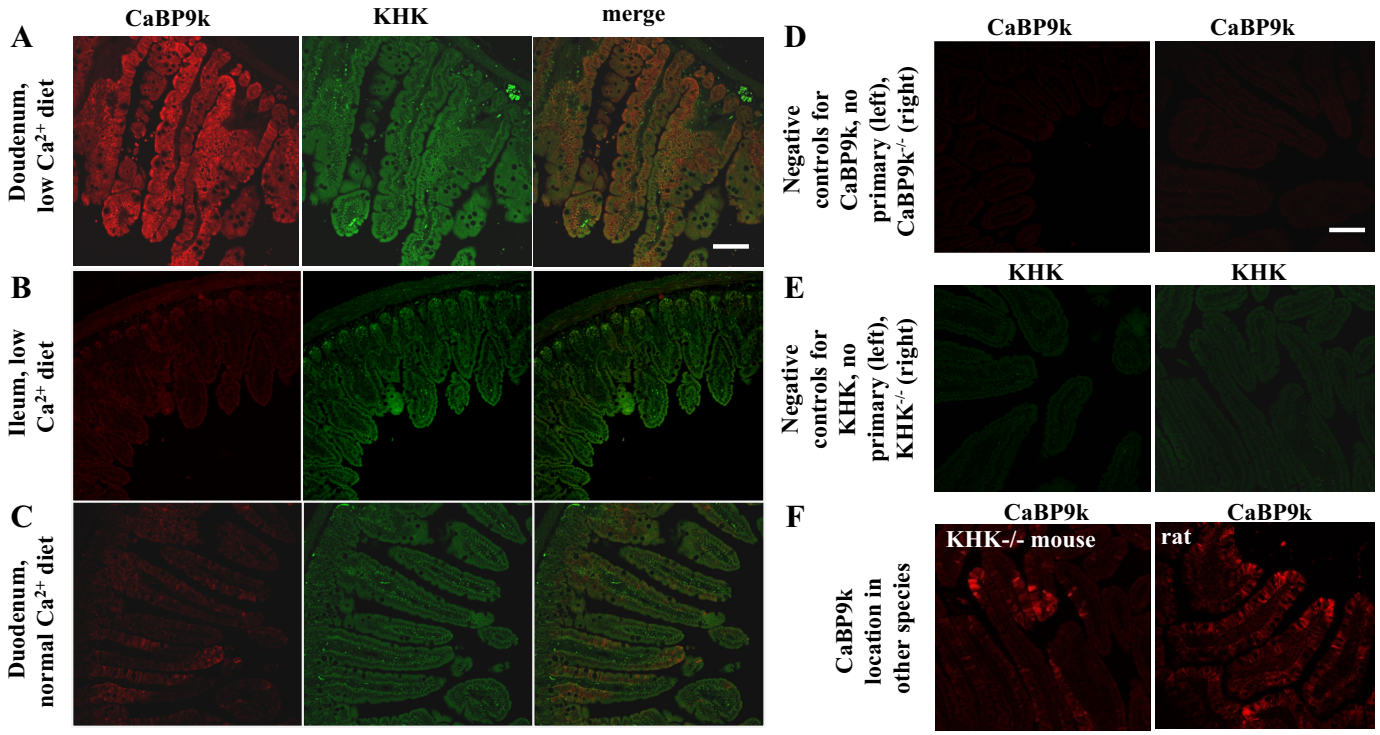

Fig. 2. Location of Ca^{2+}-binding protein D_9K (CaBP9k) and KHK along the villus. *A*: distribution of CaBP9k (*left*, red) and KHK (*middle*, green) along the entire duodenal villus of wild-type mice fed low Ca^{2+} levels. The merged panel (*right*) shows that the distribution of CaBP9k overlaps with that of KHK in most cells lining the villi of mice fed low-Ca^{2+} diets. White bar in *A* = 100 μm, images taken at ×20 magnification. Distribution of CaBP9k and KHK in the ileum (*B*) of wild-type mice fed low Ca^{2+} and in the duodenum (*C*) of wild-type mice fed normal Ca^{2+} levels. KHK distribution was not affected by dietary Ca^{2+} levels. CaBP9k expression along the intestinal crypt-villus axis of mice fed normal Ca^{2+} seems depleted and heterogeneous as indicated in the merged panel (*right*). *D*: negative control sections for CaBP9k, from wild-type mice probed with secondary antibody only (*left*) and from CaBP9k$^{-/-}$ mice probed with primary and secondary antibody. White bars in *D* and *E* = 100 μm, magnification = ×20. *E*: negative control sections for KHK, from wild-type mice probed with secondary antibody only (*left*) and from KHK$^{-/-}$ mice probed with primary and secondary antibody. Results indicate highly specific antibodies. *F*: heterogeneous, seemingly punctuate, distribution of CaBP9k along the villus axis was also found in KHK$^{-/-}$ mice (*left*) and Fischer 344 rats (*right*) fed normal Ca^{2+}. White bar = 100 μm, image taken at ×20.

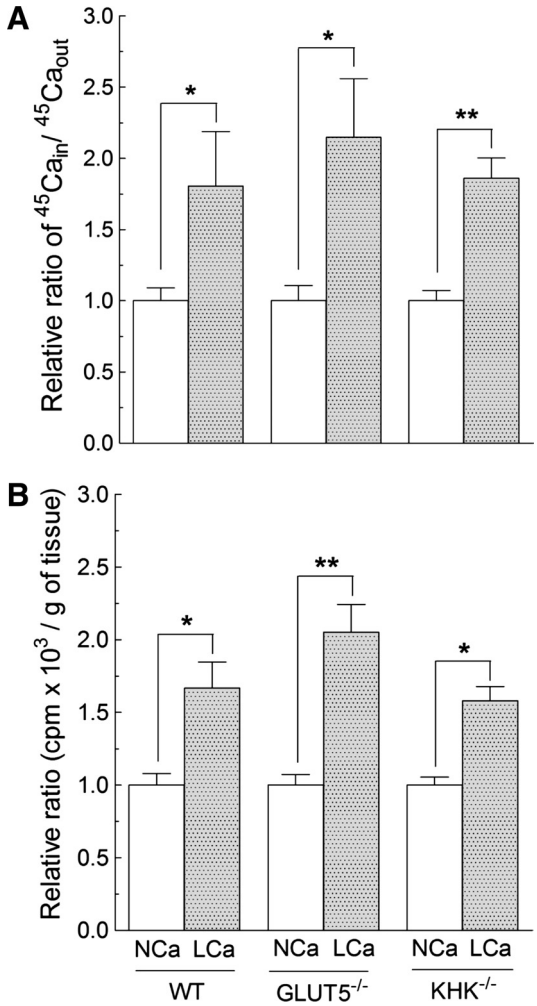

Fig. 3. Increased rates of Ca^{2+} transport after consumption of a low-Ca^{2+} diet for 4 wk. Mice were randomly divided into 2 groups then fed with normal- (NCa) or low-Ca^{2+} (LCa) diets. Because production of transgenic mice is unpredictable, 0.25 mM Ca^{2+} transport had to be determined at different times for wild-type, glucose transporter 5 (GLUT5)$^{-/-}$, and KHK$^{-/-}$ mice. Thus uptake in low Ca^{2+} was normalized to that of normal Ca^{2+} for each genotype. The composition of the solution outside the everted sac is exactly the same as that inside except tracer $^{45}Ca^{2+}$ was added to luminal side (outside the everted sac). All sacs were incubated with 10 mM fructose. *A*: relative ratios of tracer concentration inside/outside the sacs were clearly much greater in wild-type, GLUT5$^{-/-}$, and KHK$^{-/-}$ mice fed low Ca^{2+}. *B*: steady-state tissue $^{45}Ca^{2+}$ accumulation was also much greater in all mice fed low Ca^{2+}. Bars are means ± SE; $^{**}P < 0.01$; $^{*}P < 0.05$, $n = 5$–6.

GLUT5$^{-/-}$, and KHK$^{-/-}$ mice fed low-Ca^{2+} diets (Fig. 4, *A* and *B*). Protein levels of CaBP9k also seem to increase in wild-type mice fed low Ca^{2+} (compare Fig. 2, *A* and *C*). Genotype had no significant effect ($P \geq 0.06$) on TRPV6 as well as CaBP9k expression, and there was no interaction between diet and genotype ($P \geq 0.09$). PMCA1b expression was independent of dietary Ca^{2+} in wild-type mice, but, surprisingly, PMCA1b mRNA level increased slightly (~1.7-fold) with low Ca^{2+} in GLUT5$^{-/-}$ and KHK$^{-/-}$ groups (Fig. 4*C*). The effects of diet ($P < 0.001$) and genotype ($P = 0.02$) were significant, but there was no interaction ($P = 0.53$). The only Ca^{2+} transporter whose intestinal expression did not change with diet ($P = 0.80$) in any mouse model ($P = 0.12$) was NCX1 (Fig. 4*D*), and there was no interaction between these two factors ($P = 0.19$). Dietary Ca^{2+} had no effect on intestinal expression of GLUT5, GLUT2, and KHK involved in fructose transport and metabolism and of SGLT1 involved in active glucose transport (Fig. 4, *E*–*H*) (by two-way ANOVA, $P \geq 0.26$), and there was also no interaction between dietary Ca^{2+} and genotype ($P \geq 0.48$). Because GLUT5$^{-/-}$ mice did not express GLUT5 mRNA, and KHK$^{-/-}$ mice did not have KHK mRNA, the effect of genotype was highly significant ($P < 0.0001$) on GLUT5 and KHK expression (Fig. 4, *E* and *G*) but was insignificant on GLUT2 and SGLT1 expression ($P > 0.30$) (Fig. 4, *F* and *H*).

The L-type Ca^{2+} channel Ca(v)1.3 has been proposed to mediate active intestinal Ca^{2+} transport in combination with TRPV6 (20, 46), particularly because active Ca^{2+} transport is normal in TRPV6$^{-/-}$ mice (5). However, expression of Ca(v)1.3 in enterocytes is ~20- to 30-fold less than TRPV6 (data not shown), and Ca(v)1.3 levels did not significantly respond to a low-Ca^{2+} diet (Fig. 4*I*) ($P > 0.10$ by two-way ANOVA) although there seemed to be a decrease in Ca(v)1.3 expression in GLUT5$^{-/-}$ mice. There was a significant effect of genotype ($P = 0.003$), but there was no interaction between dietary Ca^{2+} and genotype ($P = 0.06$). The low expression levels contributed to the large variation in estimates of Ca(v)1.3 mRNA expression. It is not clear why Ca(v)1.3 expression decreased in GLUT5$^{-/-}$ mice although this could be a random observation expected to occur 1 out of 20 times at $P < 0.05$. Nonetheless, in wild-type, GLUT5$^{-/-}$, and KHK$^{-/-}$ mice, the significant diet-induced increase in Ca^{2+} transport is clearly paralleled by large diet-induced increases in TRPV6 and CaBP9K, but not in Ca(v)1.3, mRNA expression.

Acute fructose effects on active Ca^{2+} transport. To test the hypothesis whether fructose decreases active Ca^{2+} transport, transepithelial Ca^{2+} transport was determined in everted intestinal sacs from wild-type mice incubated in solutions containing 10 mM glucose (control) or fructose. There were significant treatment effects ($P < 0.001$ by one-way ANOVA) on transepithelial (Fig. 5*A*) and transmembrane (Fig. 5*B*) Ca^{2+} transport. Transepithelial Ca^{2+} transport was low and similar between glucose- and fructose-incubated sacs obtained from mice fed a normal-Ca^{2+} diet: 0.35 ± 0.02 and 0.36 ± 0.03, respectively. Ca^{2+} transport increased markedly ($P < 0.01$) in all mice fed low-Ca^{2+} diets, regardless of incubation solution. This diet-inducible Ca^{2+} transport was much greater ($P < 0.01$) in sacs incubated with fructose compared with those with glucose (1.45 ± 0.21 and 0.93 ± 0.08, respectively). Thus the acute effect of fructose on Ca^{2+} transport depended on whether sacs came from mice fed normal- or low-Ca^{2+} diets.

L-glutamine at 1–12.8 mM is often used as respiratory fuel to maintain enterocyte cultures (17, 56, 58, 74). Because fructose was expected to reduce ATP levels in intestinal cells and inhibit diet-induced Ca^{2+} transport, we predicted that addition of L-glutamine to the incubation media containing fructose would reverse the fructose effects. Glutamine was not added to sacs from mice fed normal Ca^{2+}, as transepithelial Ca^{2+} transport there was low, and the acute addition of fructose had similar effects as glucose (control). Glucose- and glucose+glutamine-incubated sacs from mice fed low Ca^{2+} showed similar ($P > 0.5$) rates of active Ca^{2+} transport, which were both greater than those in sacs from mice fed normal Ca^{2+}. Likewise, Ca^{2+} fluxes were also similar between sacs incubated with fructose alone and

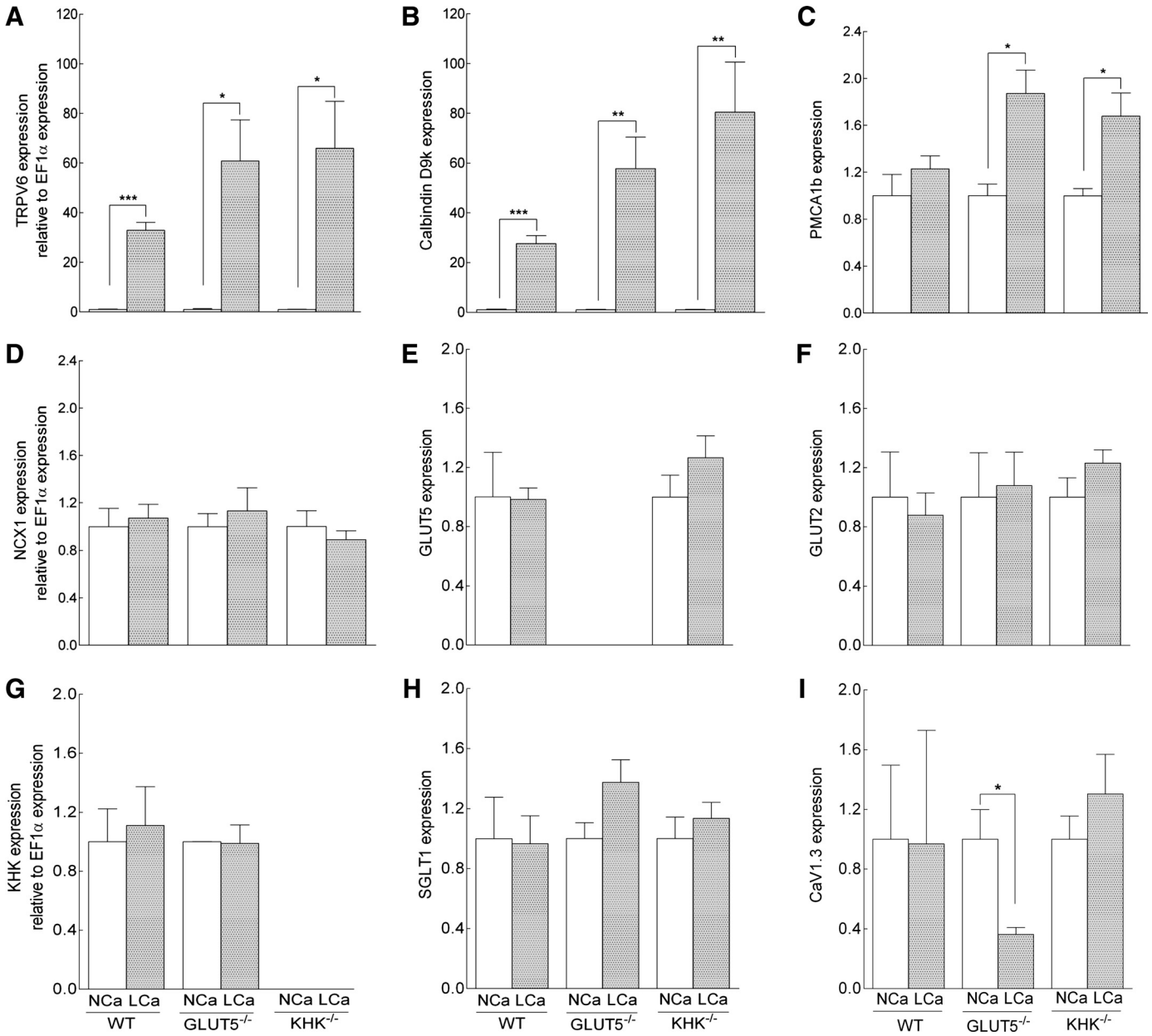

Fig. 4. The effect of low-Ca^{2+} diets on expression levels of genes involved in Ca^{2+} and fructose transport and metabolism. The mRNA expression of transient receptor potential vanilloid family calcium channel 6 (TRPV6) (*A*), CaBP9k (*B*), plasma membrane Ca^{2+}-ATPase isoform 1b (PMCA1b) (*C*), Na^+/Ca^{2+} exchanger isoform 1 (NCX1) (*D*), GLUT5 (*E*), GLUT2 (*F*), KHK (*G*), and sodium-glucose cotransporter 1 (SGLT1) (*H*, control) was examined by real-time PCR. Because recent work suggested it may also play a role in Ca^{2+} transport, expression of the L-type calcium channel Ca(v)1.3 was also determined (*I*). NCa and LCa represent normal- and low-Ca^{2+} diets, respectively. Bars are means ± SE (n = 5–6). *$P < 0.05$, **$P < 0.01$, and ***$P < 0.001$ compared with NCa in the same genotype. In contrast to TRPV6 and CaBP9k mRNA expression, which increases by orders of magnitude when a Ca^{2+}-deficient diet is consumed, Ca(v)1.3 expression does not vary with levels of dietary Ca^{2+} and with genotype, except in GLUT5$^{-/-}$ mice fed low Ca^{2+} when Ca(v)1.3 expression decreased markedly. Moreover, relative mRNA abundance of Ca(v)1.3 channels is ~20 to 30-fold less compared with that of TRPV6, and the low expression contributed to the unusually large standard error. Bars are means ± SE; n = 5–6.

those with fructose+glutamine (Fig. 5*A*). The pattern of changes in steady-state accumulation of Ca^{2+} in the mucosal tissue (Fig. 5*B*) was similar to that of active transepithelial Ca^{2+} transport. In both cases, incubation of fructose- or fructose+glutamine-incubated sacs from mice fed low Ca^{2+} still resulted in Ca^{2+} transport (or accumulation) greater than that in glucose alone- or in glucose+glutamine-incubated sacs. Thus addition of glutamine had no additional effect on diet-induced Ca^{2+} transport.

Deletion of KHK and GLUT5 did not affect diet-induced Ca^{2+} transport. Ca^{2+} uptake in the presence of fructose or glucose was determined only in mice fed low Ca^{2+}, as Fig. 3 showed all three genotypes to adaptively increase Ca^{2+} transport in response to Ca^{2+} deficiency. Because the uptake experiment could not be conducted at the same time, uptake rates in fructose-incubated sacs had to be normalized to those of glucose-incubated sacs for each mouse model (Fig. 6, *A* and *B*). The ratios of $^{45}Ca_{in}/^{45}Ca_{out}$ in glucose-incubated sacs used for

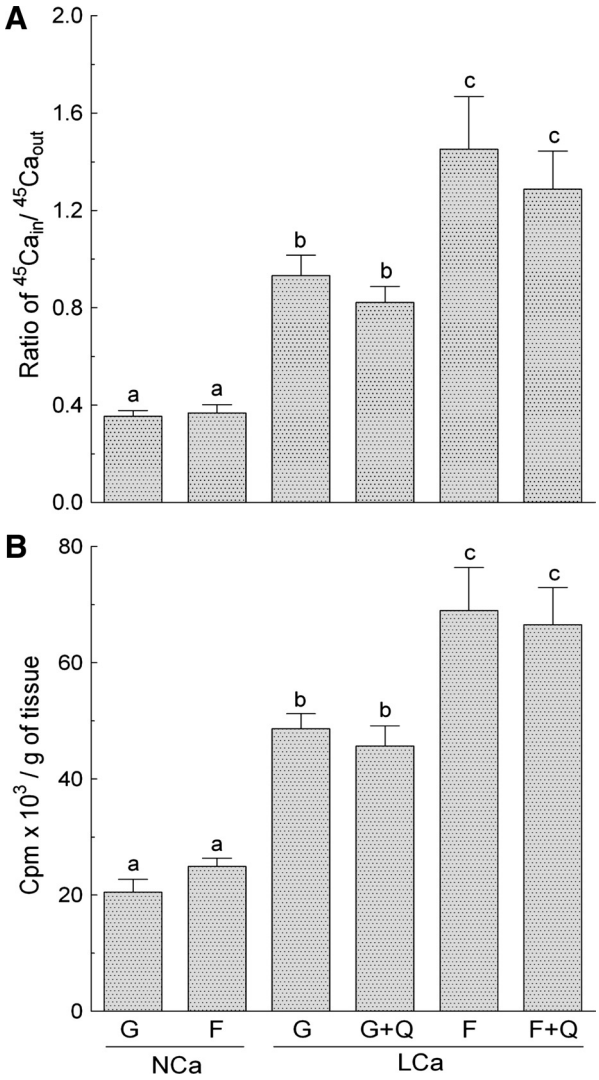

Fig. 5. The effect of sugars and L-glutamine on 0.25 mM Ca^{2+} transport (*A*) and Ca^{2+} tissue uptake (*B*). The everted sacs were incubated in 10 mM glucose (G) or fructose (F) solution and were obtained from wild-type mice fed normal- (NCa) or low-Ca^{2+} (LCa) diets for 4 wk. L-glutamine (Q, 10 mM) was added as enterocyte fuel in sacs obtained from mice fed low Ca^{2+}. The composition of the solution outside the sac is exactly the same as that inside except tracer $^{45}Ca^{2+}$ was added to luminal side (outside the everted sac). Error bars represent means ± SE (n = 4). Different letters denote significant ($P < 0.05$) differences.

normalization were 0.58 ± 0.02 for wild-type, 0.52 ± 0.05 for GLUT5$^{-/-}$, and 0.43 ± 0.02 for KHK$^{-/-}$ for Fig. 6*A*. The amounts of $^{45}Ca^{2+}$ accumulated in tissues incubated with glucose were 60.1 ± 2.5 for wild-type, 55.9 ± 1.6 for GLUT5$^{-/-}$, and 53.1 ± 11.4 × 10^3 cpm/g tissue for KHK$^{-/-}$ for Fig. 6*B*. By two-way ANOVA, there was a highly significant effect of incubation solution on transepithelial (P = 0.001) and transmembrane (P = 0.0002) Ca^{2+} transport. In both measures of Ca^{2+} transport, genotype had no effect ($P \geq 0.18$), and there was no interaction between incubation solution and genotype ($P \geq 0.70$).

Consistent with data from Fig. 5, diet-induced active Ca^{2+} transport was greater in fructose- compared with that in glucose-incubated sacs in wild-type mice. In KHK$^{-/-}$ mice, diet-induced Ca^{2+} transport was also greater in fructose- compared with glucose-incubated sacs. Interestingly, in GLUT5$^{-/-}$ mouse intestines that cannot absorb fructose (4) (C. Patel and R. Ferraris, unpublished observations), diet-induced active Ca^{2+} transport was still greater in fructose-incubated sacs. This finding suggests that fructose likely did not affect diet-induced Ca^{2+} transport because Ca^{2+} transport in the presence of fructose was similar among wild-type mice able to absorb and metabolize fructose, KHK$^{-/-}$ mice unable to metabolize fructose (41), and GLUT5$^{-/-}$ mice unable to absorb fructose. The

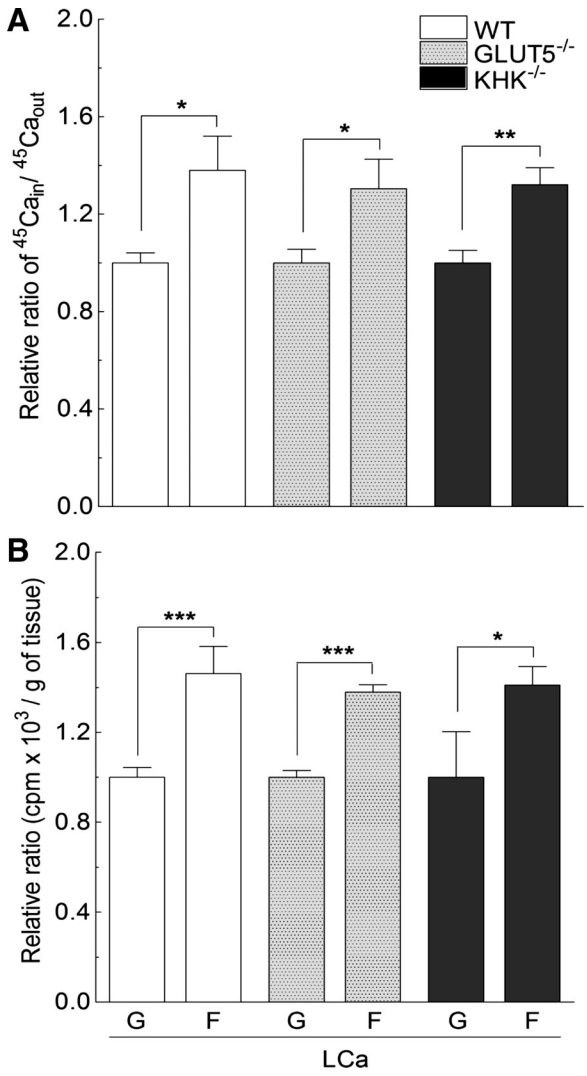

Fig. 6. The contributions of GLUT5 and KHK on sugar-modulated changes in active intestinal Ca^{2+} transepithelial transport (*A*) and Ca^{2+} tissue uptake (*B*). Wild-type, KHK$^{-/-}$, and GLUT5$^{-/-}$ mice were fed with low-Ca^{2+} diet (LCa), killed after 4 wk, and then Ca^{2+} fluxes were determined in everted sacs containing either 10 mM glucose (G) or fructose (F). Because breeding of transgenic mice is unpredictable, Ca^{2+} transport was determined at different times for wild-type (WT), GLUT5$^{-/-}$, and KHK$^{-/-}$ mice, and then Ca^{2+} uptake in fructose-incubated sacs was normalized to that in glucose-incubated, for each genotype. The composition of the solution outside the sac is exactly the same as that inside except tracer $^{45}Ca^{2+}$ was added to luminal side. Bars represent means ± SE (n = 5–6). *$P < 0.05$, **$P < 0.01$, and ***$P < 0.001$ compared with glucose-incubated sacs obtained from the same genotype. In all mice, Ca^{2+} transport was greater in sacs from fructose-fed individuals, even in GLUT5$^{-/-}$ mice, which do not absorb fructose, suggesting that perhaps the difference in Ca^{2+} transport consistently observed between glucose- and fructose-incubated sacs is due to a glucose-induced reduction of Ca^{2+} transport.

substantial difference between diet-induced Ca^{2+} transport in the presence of fructose and that in glucose probably could result from a decrease of diet-induced active Ca^{2+} transport caused by glucose. If this prediction is correct, diet-induced Ca^{2+} transport in fructose-incubated sacs of wild-type mice should be similar to that of sacs incubated with nonabsorbed sugars like mannitol, and both should be greater than Ca^{2+} transport in glucose-incubated sacs.

Diet-induced Ca^{2+} transport may be acutely inhibited by glucose metabolism. In this experiment using wild-type mice, the role of metabolism was further evaluated by determining Ca^{2+} transport in the presence of the poorly metabolizable GLUT5 substrate 2-deoxy-D-glucose and the nonmetabolized SGLT1 substrate, 3-*O*-methylglucose, as well as the nonabsorbable sugar mannitol, which represented an osmotic control (10, 18). 2-Deoxy-D-glucose can be metabolized by hexokinase but not by other glycolytic enzymes, whereas 3-*O*-methylglucose cannot be metabolized at all.

In wild-type mice fed normal-Ca^{2+} diet, the Ca^{2+} fluxes were modest but similar ($P > 0.5$) in sacs incubated with glucose and fructose solutions. Active Ca^{2+} transport was induced ($P < 0.001$ by one-way ANOVA) in five groups of mice fed low-Ca^{2+} diets. Diet-induced Ca^{2+} transport was always less ($P < 0.01$) when sacs were incubated with glucose compared with that of sacs with fructose (Fig. 7, *A* and *B*). Ca^{2+} fluxes during incubation of sacs in 2-deoxy-D-glucose, 3-*O*-methylglucose, and mannitol solutions were similar to those in fructose and were each about 50% greater than those in glucose-incubated sacs from mice fed low Ca^{2+}.

The similar effects of fructose, glucose analogs, and mannitol solutions on diet-induced active Ca^{2+} transport were confirmed in $KHK^{-/-}$ mice. Transepithelial Ca^{2+} transport in sacs from $KHK^{-/-}$ mice fed low-Ca^{2+} diets was 0.42 ± 0.04 when incubated with glucose and increased ($P < 0.05$ by one-way ANOVA) to 0.59 ± 0.06 with fructose, 0.64 ± 0.07 with 2-deoxy-D-glucose, and 0.70 ± 0.05 with mannitol ($n = 4–5$).

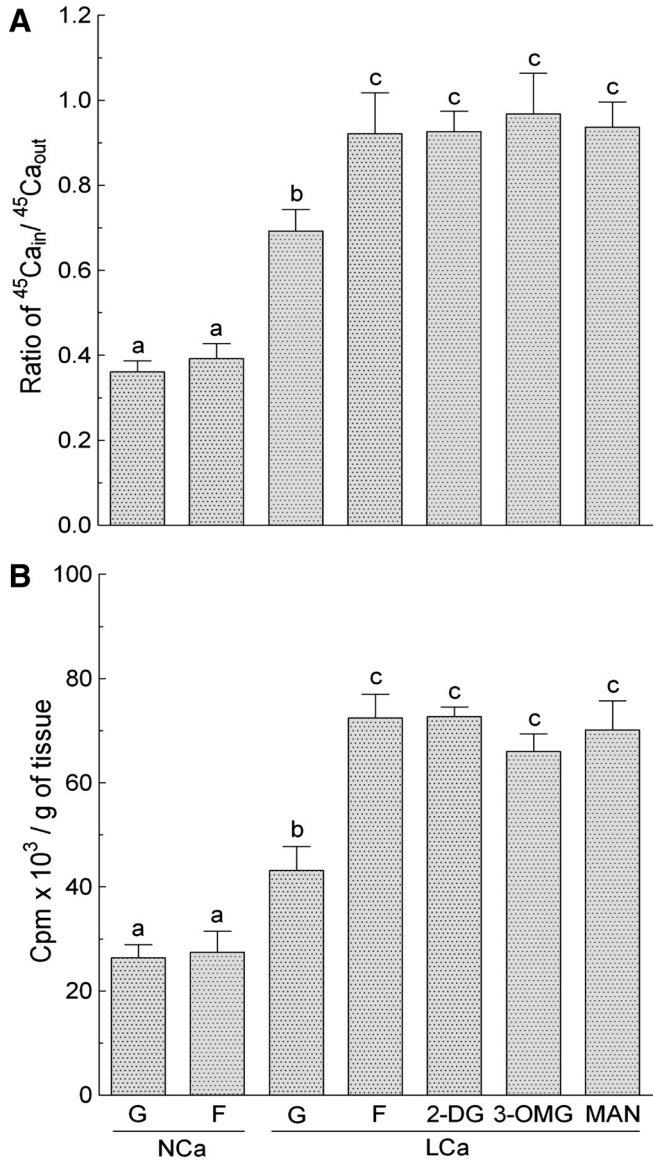

Fig. 7. The acute effects of glucose metabolism and glucose-induced transmembrane depolarization on Ca^{2+} fluxes were examined in everted sacs obtained from wild-type mice then incubated in buffer containing 10 mM glucose (G), fructose (F), 2-deoxy-D-glucose (2-DG), 3-*O*-methylglucose (3-OMG), or mannitol (MAN) on intestinal Ca^{2+} transepithelial transport (*A*) and mucosal uptake (*B*). 2DG and 3-OMG are nonmetabolized analogs of glucose that can be transported by GLUT5 and SGLT1, respectively. Mannitol is a sugar alcohol that is not transported and not metabolized. The composition of the luminal solution outside the sac is exactly the same as that inside except tracer $^{45}Ca^{2+}$ was added to luminal side. Values are means ± SE ($n = 4–6$). Different letters denote significant ($P < 0.05$) differences. A low-Ca^{2+} diet clearly induces intestinal Ca^{2+} transport. Acute incubation with glucose but not fructose, 3-OMG, 2-DG, and MAN reduces the diet-induced component of intestinal Ca^{2+} transport.

DISCUSSION

The main findings in this study are that *1*) fructose transport, fructose metabolism, and fructose-induced changes in the level of mucosal ATP have no acute effect on active, inducible intestinal Ca^{2+} transport mediated by TRPV6 and CaBP9k; *2*) glucose metabolism appears to decrease this component of intestinal Ca^{2+} transport that is inducible by a low-Ca^{2+} diet; and *3*) CaBP9k distribution may be expressed only in some intestinal cells in rodents consuming a normal-Ca^{2+} diet.

KHK and GLUT5 deletion does not affect adaptive increases in intestinal Ca^{2+} transport. When dietary Ca^{2+} concentration is nutritionally adequate, TRPV6 and CaBP9k expression is very low, suggesting that the modest Ca^{2+} transport exhibited by sacs from mice fed sufficient dietary Ca^{2+} may not be mediated by TRPV6 and CaBP9k. In contrast, dietary Ca^{2+} deficiency induces the transport and uptake of Ca^{2+}, an increase that correlated with dramatic increases in TRPV6 and CaBP9k expression. Fructose transport and metabolism do not affect these adaptive increases because a low-Ca^{2+} diet markedly upregulated Ca^{2+} transport as well as TRPV6 and CaBP9k expression in wild-type, $KHK^{-/-}$, and $GLUT5^{-/-}$ mice. We have previously shown that excessive fructose consumption by wild-type mice inhibits renal synthesis of $1,25(OH)_2D_3$, thereby compromising their ability to enhance intestinal Ca^{2+} transport during Ca^{2+} stress (21, 24, 25). Here we show that, in mice fed diets with low levels of fructose, the absence of KHK and GLUT5 does not interfere with the induction of intestinal Ca^{2+} transport by a low-Ca^{2+} diet.

Acute interactions of diet-induced, active Ca^{2+} transport with luminal fructose. Although there is an alternative hypothesis regarding fructose transport across the intestinal apical

membrane that involves, not only GLUT5, but also GLUT2 as well (47), we and others (4) found that GLUT5$^{-/-}$ mice cannot absorb fructose and would die if given dietary fructose, suggesting an absence or ineffective distribution of GLUT2 in the apical membrane and that GLUT5 is clearly the main transporter mediating fructose transport from the intestinal lumen. Fructose transport occurs mainly in the proximal regions of rat and mouse intestines (13, 61), paralleling the regional distribution of GLUT5 (22) and KHK expression, which is modestly reduced in the distal intestine. Many studies have already shown ATP concentrations to decrease markedly in enterocytes and hepatocytes exposed to fructose (33, 38, 45, 49, 54). Here we show that this well-known fructose-induced decrease in concentrations of high-energy intermediates like ATP may be highly dependent on the metabolism of fructose by KHK.

TRPV6 expression resembles that of CaBP9k and is greatest in the duodenum and corresponds to the location of the vitamin D receptor that regulates intestinal Ca^{2+} transport (57). We previously showed that active, diet-inducible Ca^{2+} transport parallels this marked proximal to distal gradient in Ca^{2+} transporter expression (21, 25). The magnitude of CaBP9k expression is directly proportional to the rate of transcellular Ca^{2+} transport, and in fact there are arguments that intracellular diffusion of Ca^{2+} bound to CaBP9k is the rate-limiting step of active Ca^{2+} transport (see review in Ref. 40). The sparse, heterogeneous distribution of CaBP9k along the villus in mice fed normal Ca^{2+} contrasts with the homogeneous distribution of KHK and suggests that some villus cells that metabolize fructose may not be capable of efficiently transporting Ca^{2+}, a condition that changes when mice are fed low Ca^{2+} as shown in Fig. 2*A*.

Although fructose transport and metabolism as well as Ca^{2+} transport can occur in the same enterocyte, diet-induced Ca^{2+} transport clearly is not affected by fructose metabolism and acute fructose-induced reductions in ATP concentrations because *1*) transcellular Ca^{2+} transport remains unchanged with or without supplementation with glutamine, a major source of respiratory fuel and metabolic energy for intestinal cells (17, 58, 74), and *2*) Ca^{2+} transport is greater in fructose- compared with glucose-incubated sacs from KHK$^{-/-}$ and GLUT5$^{-/-}$ mice.

Earlier studies directly comparing acute effects of glucose and fructose on Ca^{2+} transport in everted ileal sacs of rats seem to support our findings. Although these rats were likely fed normal-Ca^{2+} diets and high Ca^{2+} concentrations were used during incubation, transport of 45 mM Ca^{2+} was greater in 550 mM fructose than that in glucose (69). Uptake of 0.1 mM Ca^{2+}, a low concentration that favors active transcellular uptake, in 160 mM fructose was greater than that in glucose (3). Total intestinal Ca^{2+} absorption in vivo, determined acutely by femur uptake of $^{45}Ca^{2+}$, increased proportionally with increasing concentrations of honey, which is composed mostly of fructose (2).

Acute interactions of diet-induced Ca^{2+} transport with luminal glucose. Because SGLT1$^{-/-}$ mice develop glucose-galactose malabsorption syndrome (34), a condition also observed in humans with defects in SGLT1 (72), SGLT1 must be primarily responsible for glucose and galactose uptake into the intestinal cells. Glucose enters the cell via SGLT1, depolarizing the membrane, and can be metabolized in the enterocyte cytosol, which contains all enzymes involved in glycolysis (62). Glucose metabolism is dependent on luminal glucose concentrations as well as satiety state (15, 44). Because SGLT1 is expressed mainly in the enterocytes lining the villi of the proximal regions of mouse and rat intestines (30) already shown to express CaBP9k, transcellular glucose and CaBP9k-mediated Ca^{2+} transport can interact.

The inhibitory effect of glucose on diet-induced increases in Ca^{2+} transport is not due to glucose-induced changes in membrane potential reducing the downhill electrical gradient for Ca^{2+} because Ca^{2+} transport remains high in sacs incubated in 10 mM 3-*O*-methylglucose also transported by SGLT1 and thus also depolarizes the membrane (72). It is possible that glucose and 3-*O*-methylglucose have different absorption characteristics via SGLT1 and the difference in the effect on Ca^{2+} transport between the glucose- and 3-*O*-methylglucose-incubated sacs may not be solely due to the nonmetabolizable nature of 3-*O*-methylglucose but also to this difference in absorption kinetics. However, the effect of 3-*O*-methylglucose on Ca^{2+} transport is similar to those of mannitol and of 2-deoxy-D-glucose, suggesting that the different effect on Ca^{2+} transport between 3-*O*-methylglucose and glucose is less likely due to differences in absorption properties but more likely due to differences in metabolic attributes. This conclusion can be confirmed in future work in mouse models without rate-limiting glycolytic enzymes (e.g., hexokinase) and transporters (e.g., SGLT1) in the small intestine.

CaBP9k and KHK distribution along intestinal villus axis. An unexpected finding in this study is the consistently heterogeneous, seemingly punctuate, distribution of CaBP9k in the intestinal mucosa of mice and rats fed normal Ca^{2+}. The study of Lee et al. (50) and Taylor and Wasserman (64) had similar findings, but the latter ascribed the immunoreactivity to goblet cells. The heterogeneous crypt-villus distribution of CaBP9k that decreases sharply in distal intestinal regions contrasts with that of KHK, which is more homogeneous and still modestly expressed distally. Other studies found CaBP9k-immunoreactive sites to be homogeneously distributed in the villi of rabbit (39), chick (66), and human (37) intestines, so perhaps our findings are limited to mice and rats fed sufficient levels of dietary Ca^{2+}.

Feeding with low-Ca^{2+} diets seems to increase the number of CaBP9k-containing cells as well as the expression of CaBP9k protein in many cells. This is understandable because CaBP9k expression is regulated by vitamin D (8), whose levels increase with Ca^{2+} deficiency, and the vitamin D receptor appears to be homogeneously expressed in all cells lining the intestinal villi (57, 70). The heterogeneous CaBP9k distribution along the villus suggests that, in Ca-sufficient rodents, CaBP9k is not significantly expressed in some enterocytes that may have the vitamin D receptor. Future work should confirm and evaluate the graded CaBP9k response of the rodent intestine to Ca^{2+} sufficiency.

Chronic vs. acute effects of sugars on intestinal Ca^{2+} transport. We previously showed that, in rats and mice with high Ca^{2+} requirements (e.g., during lactation) or that are nutritionally deficient in Ca^{2+}, compensatory increases in 1,25-$(OH)_2D_3$-regulated intestinal Ca^{2+} absorption is strongly inhibited by chronic consumption of dietary fructose (21, 24, 25). The mechanism underlying this chronic fructose effect is a fructose-induced decrease in levels of 1α-hydroxylase, the enzyme synthesizing 1,25-$(OH)_2D_3$. Interestingly, we show in our cur-

rent study that fructose has no acute effect on diet-induced, 1,25-$(OH)_2D_3$-regulated Ca^{2+} transport; rather, glucose metabolism by enterocytes may acutely inhibit this diet-induced component of intestinal Ca^{2+} absorption. Clearly, additional studies need to be done to increase our understanding of dietary sugar-Ca^{2+} interactions, in light of increased sugar and decreased Ca^{2+} consumption by many Americans (55).

ACKNOWLEDGMENTS

This study was in partial fulfillment for a PhD in Exercise Science, Mahidol University, Thailand. We are deeply indebted to Guoqiang Wang for help in the ATP assays, Luke Fritsky for help during confocal microscopy and image analysis, Prof. Tibor Rohacs for valuable discussion regarding TRPV6, Prof. Narattaphol Charoenphandhu for valuable advice, and Prof. Sylvia Christakos for the generous gift of CaBP9k$^{-/-}$ mice.

GRANTS

This work was supported by the National Science Foundation (IOS-1121049 to R. Ferraris) and the Program Strategic Scholarships for Frontier Research Network for the Joint Ph.D. Program Thai Doctoral Degree, Office of the Higher Education Commission, Thailand (to P. Tharabenjasin).

DISCLOSURES

No conflicts of interest, financial or otherwise, are declared by the authors.

AUTHOR CONTRIBUTIONS

Author contributions: P.T., V.D., and R.P.F. conception and design of research; P.T., V.D., C.P., R.J.J., and J.Z. performed experiments; P.T., V.D., C.P., and R.P.F. analyzed data; P.T., V.D., and R.P.F. interpreted results of experiments; P.T. prepared figures; P.T. and R.P.F. drafted manuscript; P.T., V.D., C.P., N.K., R.J.J., J.Z., and R.P.F. approved final version of manuscript; V.D., N.K., R.J.J., and R.P.F. edited and revised manuscript.

REFERENCES

1. **Allen LH.** Calcium bioavailability and absorption: a review. *Am J Clin Nutr* 35: 783–808, 1982.
2. **Ariefdjohan MW, Martin BR, Lachcik PJ, Weaver CM.** Acute and chronic effects of honey and its carbohydrate constituents on calcium absorption in rats. *J Agric Food Chem* 56: 2649–2654, 2008.
3. **Armbrecht HJ, Wasserman RH.** Enhancement of Ca++ uptake by lactose in the rat small intestine. *J Nutr* 106: 1265–1271, 1976.
4. **Barone S, Fussell SL, Singh AK, Lucas F, Xu J, Kim C, Wu X, Yu Y, Amlal H, Seidler U, Zuo J, Soleimani M.** Slc2a5 (Glut5) is essential for the absorption of fructose in the intestine and generation of fructose-induced hypertension. *J Biol Chem* 284: 5056–5066, 2009.
5. **Benn BS, Ajibade D, Porta A, Dhawan P, Hediger M, Peng JB, Jiang Y, Oh GT, Jeung EB, Lieben L, Bouillon R, Carmeliet G, Christakos S.** Active intestinal calcium transport in the absence of transient receptor potential vanilloid type 6 and calbindin-D9k. *Endocrinology* 149: 3196–3205, 2008.
6. **Boass A, Lovdal JA, Toverud SU.** Pregnancy- and lactation-induced changes in active intestinal calcium transport in rats. *Am J Physiol Gastrointest Liver Physiol* 263: G127–G134, 1992.
7. **Bray GA, Nielsen SJ, Popkin BM.** Consumption of high-fructose corn syrup in beverages may play a role in the epidemic of obesity. *Am J Clin Nutr* 79: 537–543, 2004.
8. **Bronner F, Pansu D, Stein WD.** An analysis of intestinal calcium transport across the rat intestine. *Am J Physiol Gastrointest Liver Physiol* 250: G561–G569, 1986.
9. **Camara-Martos F, Amaro-Lopez MA.** Influence of dietary factors on calcium bioavailability: a brief review. *Biol Trace Elem Res* 89: 43–52, 2002.
10. **Cardaci S, Desideri E, Ciriolo MR.** Targeting aerobic glycolysis: 3-bromopyruvate as a promising anticancer drug. *J Bioenerg Biomembr* 44: 17–29, 2012.
11. **Carroll KM, Wood RJ, Chang EB, Rosenberg IH.** Glucose enhancement of transcellular calcium transport in the intestine. *Am J Physiol Gastrointest Liver Physiol* 255: G339–G345, 1988.
12. **Casirola DM, Ferraris RP.** alpha-Glucosidase inhibitors prevent diet-induced increases in intestinal sugar transport in diabetic mice. *Metabolism* 55: 832–841, 2006.
13. **Casirola DM, Ferraris RP.** Role of the small intestine in postpartum weight retention in mice. *Am J Clin Nutr* 78: 1178–1187, 2003.
14. **Chang YO, Hegsted DM.** Lactose and calcium transport in gut sacs. *J Nutr* 82: 297–300, 1964.
15. **Cherbuy C, Darcy-Vrillon B, Posho L, Vaugelade P, Morel MT, Bernard F, Leturque A, Penicaud L, Duee PH.** GLUT2 and hexokinase control proximodistal gradient of intestinal glucose metabolism in the newborn pig. *Am J Physiol Gastrointest Liver Physiol* 272: G1530–G1539, 1997.
16. **Christakos S, Dhawan P, Porta A, Mady LJ, Seth T.** Vitamin D and intestinal calcium absorption. *Mol Cell Endocrinol* 347: 25–29, 2011.
17. **Costa C, Huneau J, Tome D.** Characteristics of L-glutamine transport during Caco-2 cell differentiation. *Biochim Biophys Acta* 1509: 95–102, 2000.
18. **Cura AJ, Carruthers A.** The role of monosaccharide transport proteins in carbohydrate assimilation, distribution, metabolism and homeostasis. *Compr Physiol* 2: 863–914, 2012.
19. **Diggle CP, Shires M, McRae C, Crellin D, Fisher J, Carr IM, Markham AF, Hayward BE, Asipu A, Bonthron DT.** Both isoforms of ketohexokinase are dispensable for normal growth and development. *Physiol Genomics* 42A: 235–243, 2010.
20. **Dorkkam N, Wongdee K, Suntornsaratoon P, Krishnamra N, Charoenphandhu N.** Prolactin stimulates the L-type calcium channel-mediated transepithelial calcium transport in the duodenum of male rats. *Biochem Biophys Res Commun* 430: 711–716, 2013.
21. **Douard V, Asgerally A, Sabbagh Y, Sugiura S, Shapses SA, Casirola D, Ferraris RP.** Dietary fructose inhibits intestinal calcium absorption and induces vitamin D insufficiency in CKD. *J Am Soc Nephrol* 21: 261–271, 2010.
22. **Douard V, Choi HI, Elshenawy S, Lagunoff D, Ferraris RP.** Developmental reprogramming of rat GLUT5 requires glucocorticoid receptor translocation to the nucleus. *J Physiol* 586: 3657–3673, 2008.
23. **Douard V, Ferraris RP.** The role of fructose transporters in diseases linked to excessive fructose intake. *J Physiol* 591: 401–414, 2013.
24. **Douard V, Sabbagh Y, Lee J, Patel C, Kemp FW, Bogden JD, Lin S, Ferraris RP.** Excessive fructose intake causes 1,25-(OH)2D3-dependent inhibition of intestinal and renal calcium transport in growing rats. *Am J Physiol Endocrinol Metab* 304: E1303–E1313, 2013.
25. **Douard V, Suzuki T, Sabbagh Y, Lee J, Shapses S, Lin S, Ferraris RP.** Dietary fructose inhibits lactation-induced adaptations in rat 1,25-(OH)(2)D(3) synthesis and calcium transport. *FASEB J* 26: 707–721, 2012.
26. **Dowdle EB, Schachter D, Schenker H.** Requirement for vitamin D for the active transport of calcium by the intestine. *Am J Physiol* 198: 269–274, 1960.
27. **Favus MJ, Angeid-Backman E.** Effects of lactose on calcium absorption and secretion by rat ileum. *Am J Physiol Gastrointest Liver Physiol* 246: G281–G285, 1984.
28. **Ferraris RP, Casirola DM, Vinnakota RR.** Dietary carbohydrate enhances intestinal sugar transport in diabetic mice. *Diabetes* 42: 1579–1587, 1993.
29. **Ferraris RP, Diamond J.** Regulation of intestinal sugar transport. *Physiol Rev* 77: 257–302, 1997.
30. **Ferraris RP, Villenas SA, Hirayama BA, Diamond J.** Effect of diet on glucose transporter site density along the intestinal crypt-villus axis. *Am J Physiol Gastrointest Liver Physiol* 262: G1060–G1068, 1992.
31. **Ferraris RP, Yasharpour S, Lloyd KC, Mirzayan R, Diamond JM.** Luminal glucose concentrations in the gut under normal conditions. *Am J Physiol Gastrointest Liver Physiol* 259: G822–G837, 1990.
32. **Fleet JC, Schoch RD.** Molecular mechanisms for regulation of intestinal calcium absorption by vitamin D and other factors. *Crit Rev Clin Lab Sci* 47: 181–195, 2010.
33. **Ginsburg V, Hers HG.** On the conversion of fructose to glucose by guinea pig intestine. *Biochim Biophys Acta* 38: 427–434, 1960.
34. **Gorboulev V, Schurmann A, Vallon V, Kipp H, Jaschke A, Klessen D, Friedrich A, Scherneck S, Rieg T, Cunard R, Veyhl-Wichmann M, Srinivasan A, Balen D, Breljak D, Rexhepaj R, Parker HE, Gribble FM, Reimann F, Lang F, Wiese S, Sabolic I, Sendtner M, Koepsell H.** Na(+)-D-glucose cotransporter SGLT1 is pivotal for intestinal glucose absorption and glucose-dependent incretin secretion. *Diabetes* 61: 187–196, 2012.

35. **Gueguen L, Pointillart A.** The bioavailability of dietary calcium. *J Am Coll Nutr* 19: 119S–136S, 2000.
36. **Hanover LM, White JS.** Manufacturing, composition, and applications of fructose. *Am J Clin Nutr* 58: 724S–732S, 1993.
37. **Helmke K, Federlin K, Piazolo P, Stroder J, Jeschke R, Franz HE.** Localization of calcium-binding protein in intestinal tissue by immunofluorescence in normal, vitamin-D-deficient and uraemic subjects. *Gut* 15: 875–879, 1974.
38. **Herman RH, Stifel FB, Greene HL, Herman YF.** Intestinal metabolism of fructose. *Acta Med Scand Suppl* 542: 19–25, 1972.
39. **Hoenderop JG, Hartog A, Stuiver M, Doucet A, Willems PH, Bindels RJ.** Localization of the epithelial Ca(2+) channel in rabbit kidney and intestine. *J Am Soc Nephrol* 11: 1171–1178, 2000.
40. **Hoenderop JG, Nilius B, Bindels RJ.** Calcium absorption across epithelia. *Physiol Rev* 85: 373–422, 2005.
41. **Ishimoto T, Lanaspa MA, Le MT, Garcia GE, Diggle CP, Maclean PS, Jackman MR, Asipu A, Roncal-Jimenez CA, Kosugi T, Rivard CJ, Maruyama S, Rodriguez-Iturbe B, Sanchez-Lozada LG, Bonthron DT, Sautin YY, Johnson RJ.** Opposing effects of fructokinase C and A isoforms on fructose-induced metabolic syndrome in mice. *Proc Natl Acad Sci USA* 109: 4320–4325, 2012.
42. **Jiang L, David ES, Espina N, Ferraris RP.** GLUT-5 expression in neonatal rats: crypt-villus location and age-dependent regulation. *Am J Physiol Gastrointest Liver Physiol* 281: G666–G674, 2001.
43. **Jiang L, Ferraris RP.** Developmental reprogramming of rat GLUT-5 requires de novo mRNA and protein synthesis. *Am J Physiol Gastrointest Liver Physiol* 280: G113–G120, 2001.
44. **Jones GM, Mayer RJ.** Glucose metabolism in the rat small intestine: the effect of glucose analogues on hexokinase activity. *Biochem J* 132: 125–128, 1973.
45. **Karczmar GS, Kurtz T, Tavares NJ, Weiner MW.** Regulation of hepatic inorganic phosphate and ATP in response to fructose loading: an in vivo 31P-NMR study. *Biochim Biophys Acta* 1012: 121–127, 1989.
46. **Kellett GL.** Alternative perspective on intestinal calcium absorption: proposed complementary actions of Ca(v)1.3 and TRPV6. *Nutr Rev* 69: 347–370, 2011.
47. **Kellett GL, Brot-Laroche E, Mace OJ, Leturque A.** Sugar absorption in the intestine: the role of GLUT2. *Annu Rev Nutr* 28: 35–54, 2008.
48. **Kles KA, Wallig MA, Tappenden KA.** Luminal nutrients exacerbate intestinal hypoxia in the hypoperfused jejunum. *JPEN J Parenter Enteral Nutr* 25: 246–253, 2001.
49. **Lamers JM, Hulsmann WC.** The effect of fructose on the stores of energy-rich phosphate in rat jejunum in vivo. *Biochim Biophys Acta* 313: 1–8, 1973.
50. **Lee GS, Lee KY, Choi KC, Ryu YH, Paik SG, Oh GT, Jeung EB.** Phenotype of a calbindin-D9k gene knockout is compensated for by the induction of other calcium transporter genes in a mouse model. *J Bone Miner Res* 22: 1968–1978, 2007.
51. **Lengemann FW, Comar CL, Wasserman RH.** Absorption of calcium and strontium from milk and nonmilk diets. *J Nutr* 61: 571–583, 1957.
52. **Lengemann FW, Wasserman RH, Comar CL.** Studies on the enhancement of radiocalcium and radiostrontium absorption by lactose in the rat. *J Nutr* 68: 443–456, 1959.
53. **Manolescu AR, Witkowska K, Kinnaird A, Cessford T, Cheeseman C.** Facilitated hexose transporters: new perspectives on form and function. *Physiology (Bethesda)* 22: 234–240, 2007.
54. **Mavrias DA, Mayer RJ.** Metabolism of fructose in the small intestine. 1. The effect of fructose feeding on fructose transport and metabolism in rat small intestine. *Biochim Biophys Acta* 291: 531–537, 1973.
55. **Nicklas TA, O'Neil CE, Fulgoni VL 3rd.** The role of dairy in meeting the recommendations for shortfall nutrients in the American diet. *J Am Coll Nutr* 28, *Suppl* 1: 73S–81S, 2009.
56. **Oba M, Baldwin RLt, Bequette BJ.** Oxidation of glucose, glutamate, and glutamine by isolated ovine enterocytes in vitro is decreased by the presence of other metabolic fuels. *J Anim Sci* 82: 479–486, 2004.
57. **Palm C, Hartmann K, Weber K.** Expression and immunolocalization of calcium transport proteins in the canine duodenum, kidney, and pancreas. *Anat Rec (Hoboken)* 293: 770–774, 2010.
58. **Porteous JW.** Intestinal metabolism. *Environ Health Perspect* 33: 25–35, 1979.
59. **Schachter D, Dowdle EB, Schenker H.** Active transport of calcium by the small intestine of the rat. *Am J Physiol* 198: 263–268, 1960.
60. **Schuette SA, Knowles JB, Ford HE.** Effect of lactose or its component sugars on jejunal calcium absorption in adult man. *Am J Clin Nutr* 50: 1084–1087, 1989.
61. **Solberg DH, Diamond JM.** Comparison of different dietary sugars as inducers of intestinal sugar transporters. *Am J Physiol Gastrointest Liver Physiol* 252: G574–G584, 1987.
62. **Srivastava LM, Hubscher G.** Glucose metabolism in the mucosa of the small intestine. Glycolysis in subcellular preparations from the cat and rat. *Biochem J* 100: 458–466, 1966.
63. **Suzuki T, Douard V, Mochizuki K, Goda T, Ferraris RP.** Diet-induced epigenetic regulation in vivo of the intestinal fructose transporter Glut5 during development of rat small intestine. *Biochem J* 435: 43–53, 2011.
64. **Taylor AN, Wasserman RH.** Immunofluorescent localization of vitamin D-dependent calcium-binding protein. *J Histochem Cytochem* 18: 107–115, 1970.
65. **Thorens B, Mueckler M.** Glucose transporters in the 21st Century. *Am J Physiol Endocrinol Metab* 298: E141–E145, 2010.
66. **Thorens B, Roth J, Norman AW, Perrelet A, Orci L.** Immunocytochemical localization of the vitamin D-dependent calcium binding protein in chick duodenum. *J Cell Biol* 94: 115–122, 1982.
67. **Turner JD, Gaspers LD, Wang G, Thomas AP.** Uncoupling protein-2 modulates myocardial excitation-contraction coupling. *Circ Res* 106: 730–738, 2010.
68. **van den Berghe G, Bronfman M, Vanneste R, Hers HG.** The mechanism of adenosine triphosphate depletion in the liver after a load of fructose. A kinetic study of liver adenylate deaminase. *Biochem J* 162: 601–609, 1977.
69. **Vaughan OW, Filer LJ Jr.** The enhancing action of certain carbohydrates on the intestinal absorption of calcium in the rat. *J Nutr* 71: 10–14, 1960.
70. **Wang Y, Zhu J, DeLuca HF.** Where is the vitamin D receptor? *Arch Biochem Biophys* 523: 123–133, 2012.
71. **Woods HF, Eggleston LV, Krebs HA.** The cause of hepatic accumulation of fructose 1-phosphate on fructose loading. *Biochem J* 119: 501–510, 1970.
72. **Wright EM, Loo DD, Hirayama BA.** Biology of human sodium glucose transporters. *Physiol Rev* 91: 733–794, 2011.
73. **Wu X, Wang X, Gao J, Yu Y, Jia S, Zheng J, Dallos P, He DZ, Cheatham M, Zuo J.** Glucose transporter 5 is undetectable in outer hair cells and does not contribute to cochlear amplification. *Brain Res* 1210: 20–28, 2008.
74. **Yang H, Soderholm JD, Larsson J, Permert J, Lindgren J, Wiren M.** Bidirectional supply of glutamine maintains enterocyte ATP content in the in vitro using chamber model. *Int J Colorectal Dis* 15: 291–296, 2000.
75. **Younoszai MK, Nathan R.** Intestinal calcium absorption is enhanced by D-glucose in diabetic and control rats. *Gastroenterology* 88: 933–938, 1985.